

Threading the Needle: Fluorescent Poly-*pseudo*-rotaxanes for Size-Exclusion Sensing

Niamh Willis-Fox,^{1,2} Christian Belger,² Rachel C. Evans*¹ and Timothy M. Swager*²

1 School of Chemistry, Trinity College Dublin, Dublin 2, Ireland

2 Department of Chemistry and The Institute of Soldier Nanotechnologies, Massachusetts Institute of Technology, 77 Massachusetts Avenue, Cambridge, MA 02139, USA.

Abstract:

Poly-*pseudo*-rotaxanes have been formed through the threading of cucurbit[n]urils (**CB[n]**) onto the cationic electron-poor poly(pyridyl vinylene), **PPyV**. The threading of **CB[n]** onto the **PPyV** backbone is confirmed by a broadening and upfield shift in the **PPyV** ¹H NMR signals. Encapsulation of **PPyV** within the **CB[n]** macrocycles produces dramatic fluorescence enhancements with improved solubility. The threading ability of the **CB[n]** on the **PPyV** backbone is governed by the dimensions of the particular **CB[n]** portal, which grows with increasing number of methylene-bridged glycoluril repeat units. **CB[5]** is too small to thread onto the **PPyV** backbone. The portal of **CB[6]** requires extra time suggesting high preorganization and/or macrocycle deformation are required to thread onto **PPyV**. Alternatively the portal of **CB[8]** appears to be large enough such that it doesn't have sufficiently large dipole-dipole interactions with the **PPyV** chain to promote a strong threading equilibrium. However we find that the portal of **CB[7]** is optimal for the threading of **PPyV**. The **PPyV-CB[n]** system was further exploited to demonstrate a dual-action sensor platform, combining the PL-responsive behaviour demonstrated by **PPyV** towards electron-rich analytes with the size-exclusion properties imparted by volume of the respective **CB[n]** cavities. Thin films of **PPyV-CB[7]** were found to display reversible photoluminescence quenching when exposed to vapours of the biologically relevant molecule indole which is recovered under ambient conditions, suggesting prospects for new size-exclusion based selective sensory schemes for volatile electron-rich analytes.

Introduction:

Semiconducting conjugated polymers (CP) are low cost solution processability materials with applications ranging from photovoltaics,^{1, 2} polymer light-emitting devices,^{3, 4} to optical sensors.^{5, 6} The innate ability of CPs to transport excitons over large distances offers great potential to amplify signals in fluorescent sensors,⁷ with the majority of photoluminescence (PL) sensor platforms being electron-donating polymers for the detection of electron-accepting analytes.^{5, 6, 8-11} The alternative, or inverse situation utilizing electron-accepting (n-type) semiconducting polymers, is limited by few available materials.¹²⁻¹⁷ However, despite the scarcity in reports with n-type CPs, this class of materials has been identified as being critical to applications including polymeric solar cells¹⁸ and organic light-emitting diodes.¹⁵ Approaches to n-type CPs involve the addition of highly electron-withdrawing species such as fluorinated groups^{19, 20} or the introduction of electron-deficient heterocyclic aromatics into the polymer backbone.^{12, 13} Recently, poly(pyridinium phenylene)s have been developed that show selectively to biologically important species such as indole, through oxidative electron-transfer quenching of the photoluminescence.¹⁶ Cationic conjugated n-type polymers have further shown tunability by simply exchanging the counter anions.¹⁷ These CPs demonstrated the ability to selectively detect industrially relevant amine vapours at or below permissible exposure limits.

Rotaxane systems are effective sensing platforms for a wide range of charged guest species using optical transduction process.^{21, 22} A rotaxane is defined as a physically interlocked structure containing a linear molecular axle threaded through a macrocycle and locked in place by large terminal bulky stopper groups.²³ Systems lacking the stopper groups can have similar structures, but because they can disassemble they are referred to as *pseudo*-rotaxanes.²⁴ Polyrotaxanes, wherein a number of cyclic units are threaded onto a linear chain, have been demonstrated as effective sensing elements²⁵ with particular use in biotechnology due to their low cytotoxicity.²⁴ A combination of the molecular recognition bestowed by the host-guest polyrotaxane interactions and amplified response by excitation migration in conjugated polymers have previously been used to produce highly selective sensing schemes for Cu⁺ ions.^{26, 27}

We report herein polyrotaxane systems based on n-type CP threaded through macrocycles of varying sizes to detect electron-rich analytes. The macrocycles chosen for this work are a series of highly symmetrical molecules known as cucurbit[*n*]urils (CB[*n*]), which are known to bind protonated nitrogen heterocycles and have solubility of 700 mM in 50/50 *v/v* formic acid/H₂O.²⁸ In cucurbit[*n*]urils glycoluril units are arranged such that the carbonyl dipoles define portals to an interior hydrophobic cavity.²⁹ CB[*n*]s exhibit selective binding of both neutral and positively charged guest species,^{28, 29} and can also discriminate between a range of aliphatic and aromatic species.³⁰⁻³² Our interest in threading CPs with CB[*n*]s is to exploit this discriminating binding with the sensitivity afforded by exciton migration to create a new fluorescence quenching and size-exclusion sensory platform. To this end, we report the self-assembly of poly-*pseudo*-rotaxanes by threading of cucurbit[*n*]urils (CB[5]-CB[8]) onto the backbone of a cationic electron-poor conjugated polymer poly(pyridyl vinylene), **PPyV** (**Fig. 1**). ¹H NMR and fluorescence spectroscopies have been employed to determine the effect the size of the portal cavity has on **PPyV-CB[*n*]** interactions. We demonstrate that **PPyV** displays dramatic fluorescence enhancements upon encapsulation within the **CB[*n*]** species. We show that the size of the **CB[*n*]** portal of the poly-*pseudo*-rotaxanes can be exploited to develop a size-exclusion based fluorescence sensing platform for biologically-important electron-rich analytes both in solution and solid state.

Results and Discussion:

CB[*n*]s have a high affinity for positively charged guest species largely through synergistic hydrophobic and dipole-dipole interactions.^{28, 29} The strength of these interactions along with the size of the individual cucurbit[*n*]urils is expected to control the extent of threading onto the **PPyV** backbone (**Fig. 1**). The dimensions of the **CB[*n*]** species, outlined in **Table 1**, are controlled by the varying number of glycoluril units possessed by each **CB[*n*]**. Of particular importance is the diameter (*a*) of the carbonyl lined **CB[*n*]** portal, the equatorial width (*b*), the height (*c*), and interior volume (*V*).

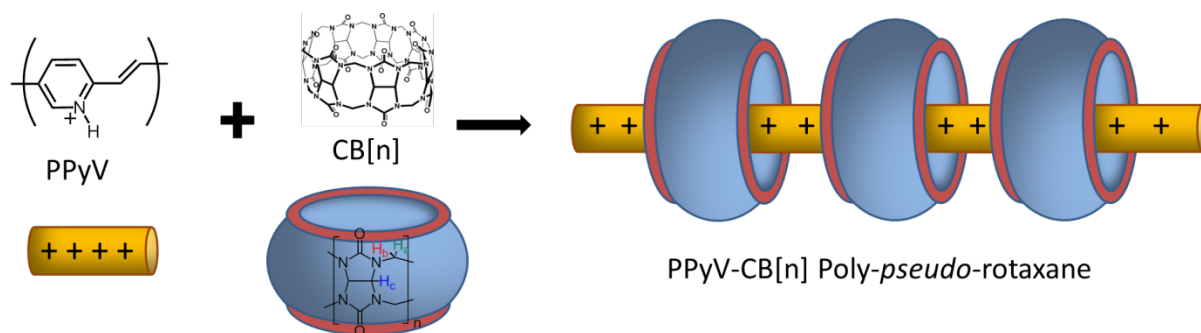


Figure 1. Schematic representation of poly-*pseudo*-rotaxane formation *via* binding of positively charged repeat units of **PPyV** by a host cucurbit[*n*]uril macrocycle.

Table 1. Physical properties and dimensions of **CB[n]** series used in this study.^{28, 29}

	M_w (g mol^{-1})	a (Å)	b (Å)	c (Å)	V (Å ³)
CB[5]	830	2.4	4.4	9.1	82
CB[6]	996	3.9	5.8	9.1	164
CB[7]	1163	5.4	7.3	9.1	279
CB[8]	1329	6.9	8.8	9.1	479

Threading of **CB[n]** onto the **PPyV** backbone

The threading of **CB[n]** onto the **PPyV** backbone was confirmed using ¹H NMR spectroscopy in D₂O/*d*₂-formic acid 50/50 *v/v*. The ¹H NMR spectrum of **PPyV** exhibits five distinct signals between 6.2-7.8 ppm, the assignment for which can be found in **Fig. S1a**, Supporting Information. In general, encapsulation of a guest molecule within a **CB[n]** cavity causes an upfield shift of the guest protons. Alternatively protons located at the portal of the **CB[n]** undergo a downfield shift as they experience a deshielding effect from the carbonyl groups surrounding the cavity opening.^{28, 29} The ¹H NMR spectrum of **PPyV** as a function of increasing **CB[n]** concentration is shown in **Fig. 2a**. On increasing the **CB[7]** concentration a broadening and an upfield shift is observed for all of the **PPyV** protons, attributed to threading of the **PPyV** backbone by **CB[7]**. A similar broadening and upfield shift is observed for **CB[6]** (**Fig. S2**), again consistent with a threading of the **PPyV** backbone by the cucurbituril. **CB[8]** showed poor solubility at concentrations required to measure NMR experiments and so dilute samples were used. Although the spectra provide limited resolution, we detect weak signals that experience broadening and upfield shifts supporting a threaded **PPyV** backbone (**Fig. S3**). By comparison, the addition of **CB[5]** to **PPyV** results in no signal broadening or upfield shift

exhibited by the **PPyV** proton signals (**Fig. 2b**), indicating that **CB[5]** does not thread onto the CP backbone. Thus, **CB[5]** can be thought of as a *pseudo* control species as it represents the addition of a cucurbit[*n*]uril that does not bind to the **PPyV** backbone.

The three signals seen at 4.5, 2.9 and 4.2 ppm in the ^1H NMR spectrum (**Fig. S1b**) are assigned to the H_a , H_b and H_c ³³⁻³⁵ protons of the unbound **CB[n]**, respectively. At low concentrations, the addition of **CB[7]** to **PPyV** causes these three proton signals to be shifted upfield (**Fig. S4**). At a ratio of 20 **PPyV** r.u. to 1 **CB[7]**, a signal appears at 4.20 ppm with a shoulder at 4.25 attributed to H_c in the bound and unbound forms of **CB[7]**, respectively. Also at this concentration the signal at 2.90 ppm becomes unresolvable as a doublet as a result of the close proximity of the signals attributed to H_b for both bound and unbound **CB[7]**. As the concentration of **CB[7]** increases, the contributions from the signals of the unbound **CB[7]** increase and swamp the signal of the bound **CB[7]**. This indicates that the binding of **CB[7]** with **PPyV** does not scale linearly with **CB[7]** concentration and saturation occurs at reasonably low concentrations (between 20:1 and 10:1 **PPyV** r.u. to **CB[n]**).

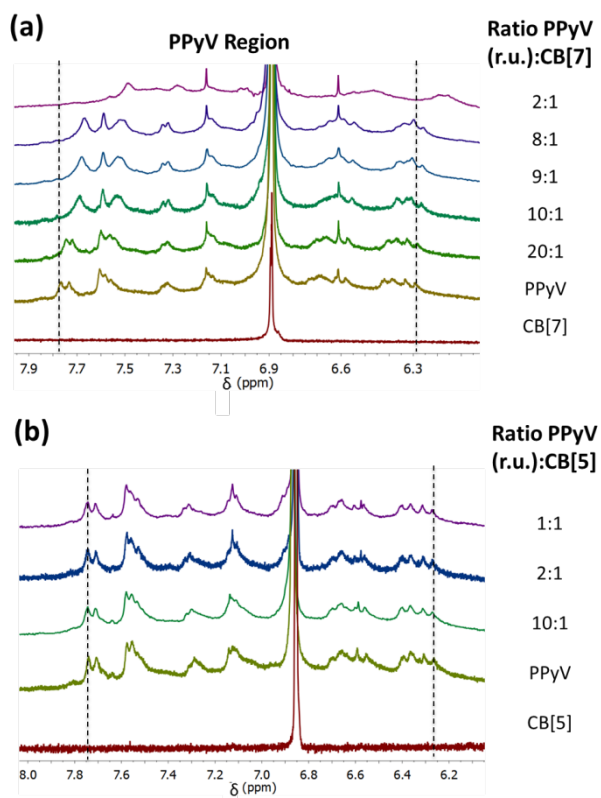


Figure 2. ^1H NMR spectra for **PPyV** with increasing concentration of (a) **CB[7]** and (b) **CB[5]** in 50/50 v/v $\text{D}_2\text{O}/d_2$ -formic acid at 298 K.

Fluorescence Enhancement of PPyV on threading of CB[n]

A number of reports have observed enhancement in the fluorescence of guest species on formation of inclusion complexes with cucurbit[n]urils.^{31, 36, 37} Thus, steady-state emission measurements were carried out below the saturation concentrations determined in our NMR studies to investigate the effect of threading of **CB[n]** onto the **PPyV** backbone on the PL properties. The PL spectrum of **PPyV** in concentrated formic acid shows a broad band between 430-610 nm with a maximum at 480 nm as previously reported.³⁸ **PPyV** is sparingly soluble in water and thus, increasing the water content to the 50/50 v/v H₂O/formic acid solution in which the **CB[n]** species are soluble, causes a decrease in PL intensity and a red shift in the observed emission maximum (**Fig. S5**), which is indicative of increasing polymer aggregation.³⁹ Changes in the PL spectrum of **PPyV** on addition of each of the **CB[n]**s are shown in **Fig. 3**. A dramatic enhancement in the PL intensity is observed for **CB[6]**, **CB[7]** and **CB[8]**, the magnitude of which is dependent on the dimensions of the **CB[n]**. Previously the enhancement of the PL signal observed on binding of a guest species within a **CB[n]** host has been attributed to increasing the guest solubility and changing the polarity of the microenvironment.^{37, 40, 41} Titration of **CB[5]** into **PPyV** gives rise to little or no change to the PL spectrum. This further confirms the evidence from the ¹H NMR studies which indicates that **CB[5]** does not thread the **PPyV** backbone. The fact that **CB[5]** does not thread onto the **PPyV** backbone was expected as the dimensions of the portal opening and cavity cause it to be unable to bind anything larger than a proton or a very small positively charged ion such as an ammonium moiety at its portal.²⁸ The diameter of pyridine, the major component of **PPyV** is reported to be 4.92 Å parallel to the C_{2v} axis and 5.12 Å perpendicular to this axis in the plane of the molecule.⁴² It is clear that the portal diameter of **CB[5]** (2.4 Å) is too small to thread onto the aromatic backbone of **PPyV** and thus it cannot influence the microenvironment of the chromophoric segments of the **PPyV** polymer chain to bring about the increase in PL intensity observed for the three larger **CB[n]**s.

The dimensions of the **CB[n]** portal and cavity not only control the ability of the **CB[n]** to thread onto the **PPyV** backbone, but also influence the magnitude of the concomitant PL with respective enhancements **CB[6] < CB[8] < CB[7]**. The PL enhancement of **PPyV-CB[6]** requires ~2 hr to reach a maximum intensity after **CB[6]** addition. However, the PL enhancement is virtually

instantaneous on addition of **CB[7]** or **CB[8]** (Fig. S6). **CB[6]** has previously been reported to bind linear hydrocarbons,³¹ and smaller aromatic molecules.⁴³ In contrast **CB[7]** and **CB[8]** have both been shown to easily encapsulate aromatic molecules⁴⁴ with the larger portal of **CB[8]** capable of binding two aromatic molecules.²⁸ The binding of any of these species relies heavily on dipole-dipole interactions between the cationic nature of the guest species and the carbonyl groups that decorate each of the cavity openings and through hydrophobic interactions.²⁹ Based on these observations we propose the smaller portal diameter of **CB[6]** (3.9 Å) requires more preorganization that slows the kinetics of **PPyV** threading. Specifically with larger guest species that match or are larger than the **CB[6]** portal, significant deformation of the macrocycle has been suggested as an explanation for the slower incorporation of target molecules.^{45, 46} The portal diameter of **CB[8]**, 6.9 Å, is larger than needed, thus it threads **PPyV** easily, but the weakened dipole-dipole interactions with the **PPyV** also leads to competitive dethreading. **CB[7]**'s portal diameter of 5.4 Å, is optimally matched to **PPyV** and the strong interactions keep **PPyV** in a threaded state. This behaviour is similar to oxazine dye binding within the cavity of **CB[7]** and **CB[8]**, wherein **CB[7]** was shown to undergo a stronger binding to the oxazine dye than the **CB[8]** host as a result of a better matched portal diameter.⁴⁴

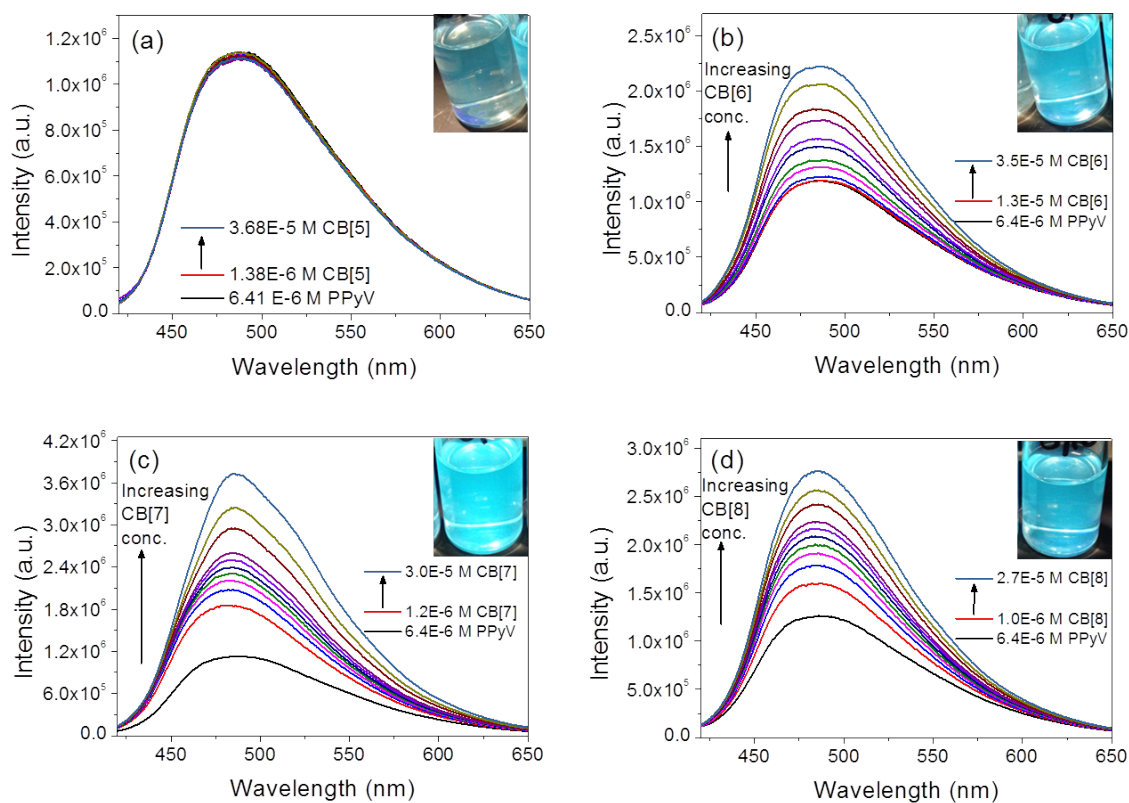


Figure 3. PL spectra ($\lambda_{\text{ex}} = 403 \text{ nm}$) of **PPyV** ($6.4 \times 10^{-6} \text{ M}$ (r.u.)) in formic acid/H₂O 50/50 *v/v* upon increasing concentration of (a) **CB[5]** (b) **CB[6]** (c) **CB[7]** and (d) **CB[8]**. The insets show photographs of the final **PPyV-CB[n]** solutions following each titration under UV-illumination ($\lambda_{\text{ex}} = 365 \text{ nm}$).

PPyV-CB[n] Quenching by Electron Rich Analytes

Previously, the high excited-state electron affinity of cationic, high ionization potential conjugated polymers has been exploited to develop PL-based sensor materials for biologically important electron-rich analytes.^{14, 17} **PPyV** is no different as the PL was found to be quenched in the presence of indole which was chosen as a result of its biological significance as the aromatic portion of the essential amino acid tryptophan. Similarly, the size of the **CB[n]** cavity has demonstrated utility as a sensing platform through binding of two complimentary guests.³⁰ Additionally, size employing different **CB[n]** portal dimensions can produce biomimetic self-sorting systems.^{47, 48} To explore the possibility of combining the PL-responsive behaviour of **PPyV** and the size controlled interactions of **CB[n]** to produce a sensor platform we performed steady-state PL quenching studies with the electron-donating species indole. The change of PL intensity of **PPyV-CB[n]** upon titration with indole and the corresponding Stern-Volmer plots are shown in **Fig. 4**. The quenching efficiencies were determined by the Stern-Volmer quenching constant, K_{sv} , which are shown in **Fig. 4**. The K_{sv} values follow the order **CB[8]**>**CB[7]**>**CB[6]** and scale with the ability of the **CB[n]**s to incorporate both **PPyV** and the electron-rich indole analyte. **CB[8]** shows ample ability to comfortably bind two aromatic species, particularly if they possess complimentary electrostatic profiles²⁸ as is the case with protonated **PPyV** and indole. **CB[7]** on the other hand does not effectively bind two aromatic species²⁸ as evidenced by its reduced K_{sv} value. Quenching in the **PPyV-CB[6]** system is almost non-existent as **CB[6]** is best matched to the binding of aliphatic amines²⁸ and an already distorted structure with the **PPyV** guest cannot incorporate a second aromatic species.

We also considered the possibility that the quenching in the **PPyV-CB[n]** systems is governed by the extent of **CB[n]** threading onto the **PPyV** backbone and the quantity of the backbone that is left exposed outside of the **CB[n]** cavity is responsible for interacting with indole. The magnitude of the PL enhancement of **PPyV** on addition of the cucurbit[*n*]uril is an indication of the

extent of **CB[n]** threading onto the **PPyV** backbone and follows the order **CB[7]>CB[8]>CB[6]>>CB[5]**. Consequently the volume of the exposed or unthreaded **PPyV** backbone follows the order **CB[5]>>CB[6]>CB[8]>CB[7]**. Thus, if the quenching were controlled by the free or unthreaded backbone available to interact with the analyte the quenching constants would follow the order **CB[6]>CB[8]>CB[7]**, which is not the case.

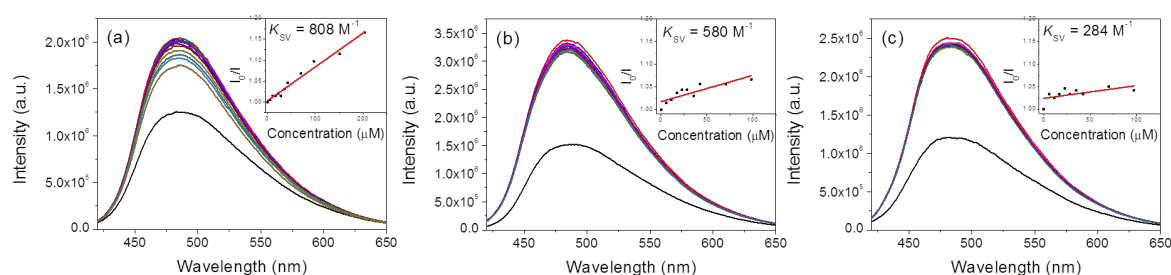


Figure 4. PL spectra of **PPyV** in formic acid/H₂O 50/50 v/v with (a) **CB[8]** (b) **CB[7]** and (c) **CB[6]** as a function of increasing indole concentration. The insets show the Stern-Volmer plots for each of the respective **PPyV-CB[n]** titrations with indole.

To further probe the role of cavity size on the quenching behaviour of the **PPyV-CB[n]** system, the PL response was determined with the smaller electron-rich analyte, *N*-methyl pyrrole. The K_{sv} for titration of *N*-methyl pyrrole with **PPyV-CB[7]** and **PPyV-CB[8]** was found to be equal (**Fig. S7**). This result is consistent with the idea that the quenching of the **PPyV-CB[n]** system is governed by the volume available within the **CB[n]** cavity following threading onto the **PPyV** backbone. The smaller size of *N*-methyl pyrrole allows it easier access into the cavities of both **CB[7]** and **CB[8]** to bring about similar quenching rates.

PPyV-CB[n] Quenching Studies in Thin Films

Each of the **PPyV-CB[n]** systems discussed are *pseudo*-rotaxanes as a result of the fact that the **CB[n]** rings are not irreversibly trapped on the **PPyV** backbone. Reduced solid state motility can equivalently physically lock the **CB[n]** rings in place on the **PPyV** backbone, and hence **PPyV-CB[n]** thin films were deposited onto glass slides. The PL maximum of **PPyV** thin films deposited from formic acid/H₂O 50/50 v/v ($\lambda_{em\ max} = 580\ nm$) are considerably red-shifted compared to the solution spectrum ($\lambda_{em\ max} = 485\ nm$). The magnitude of this shift matches that previously reported for deposition of thin films of similar cationic conjugated polymers.¹⁷ The red-shift in PL maximum of

CPs is attributed to increased aggregation in the solid-state.³⁹ The dramatic PL enhancement observed in solution for **PPyV** on addition of **CB[n]** can be transferred to the solid state and the thin film PL maximum of **PPyV-CB[7]**, shown in **Fig. 5** is blue-shifted ($\lambda_{em\ max} = 545\text{ nm}$) when compared to the **PPyV** film. Therefore, threading of **CB[7]** causes reduced aggregation of **PPyV** in the solid-state.

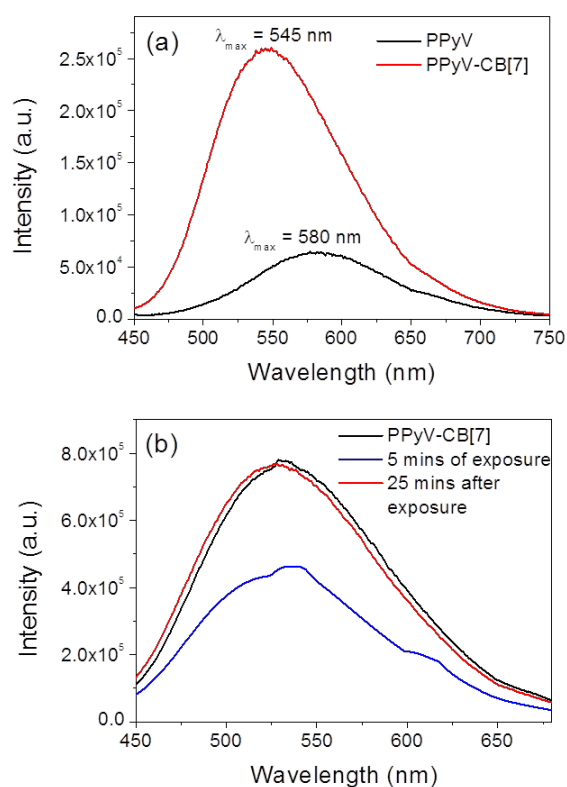


Figure 5. PL spectra ($\lambda_{ex} = 403\text{ nm}$) for (a) thin films of **PPyV** (black line) and **PPyV-CB[7]** (1:1 **PPyV** r.u. to **CB[n]**) (red line) deposited on glass and (b) a thin film of **PPyV-CB[7]** (1:25 **PPyV** r.u. to **CB[n]**) at $t = 0\text{ mins}$, after 5 mins of exposure to indole vapour and 25 min after removal of indole source and recovery in ambient conditions.

These thin films are also capable of sensing indole in the gaseous phase. After exposing a thin film of **PPyV-CB[7]** (25 **CB[n]** rings to 1 **PPyV** r.u.) to the vapour from a solution of indole (1 mg/ml in formic acid/H₂O 50/50 v/v) for 5 min, the PL intensity dropped to ~50% of the initial film intensity. The initial intensity is recovered within 25 mins after the removal of the indole vapour (**Fig. 5**). This is a promising indication of the potential for these **PPyV-CB[n]** systems to be used as simple reversible sensors for gaseous electron-rich analytes.

Conclusion:

In summary we have demonstrated the formation of poly-*pseudo*-rotaxanes through the threading of **CB[n]**s onto the cationic backbone of **PPyV**. The ability of the **CB[n]** to thread the CP backbone is governed by the portal dimensions of the **CB[n]**s. Threading of the **CB[n]** onto the **PPyV** backbone produces dramatic fluorescence enhancements and increased solubility of the **PPyV**. The smaller size of **CB[5]** precludes threading onto the CP backbone. The portal of **CB[6]** is smaller than is optimal and deformation slows the threading of **PPyV**. Alternatively the portal of **CB[8]** is larger than necessary and although it threads onto **PPyV** it suffers from fast dethreading. The portal of **CB[7]** is properly matched to **PPyV** and displays the most robust poly-*pseudo*-rotaxane structure. The electron-poor nature of **PPyV** endows these systems with fluorescence quenching responses to electron-rich bioanalytes. Combining the PL-responsive behaviour demonstrated by **PPyV** and the controlled size interactions of **CB[n]** produces a sensor platform that has utility in differentiating analytes. Thin films of **PPyV-CB[7]** display reversible quenching of the PL intensity when exposed to indole vapour under ambient conditions, suggesting prospects for new size-exclusion based selective sensory schemes for volatile electron-rich analytes.

Experimental:

Materials:

Formic acid (>95%), 4-dodecylbenzene sulfonic acid (DBSA) (≥95%), *m*-cresol (≥98%), sodium hydroxide (1 M), indole (≥99%) and *n*-methyl pyrrole (≥99%) were purchased from Sigma and were used as received. Cucurbit[5]uril, cucurbit[6]uril, cucurbit[7]uril and cucurbit[8]uril were purchased from Strem Chemicals, Inc. and were used without further purification. Deuterium oxide (D₂O) and deuterated formic acid (*d*₂-formic acid) was purchased from Cambridge Isotope Laboratories, Inc. and used as received. Poly (pyridyl vinylene) (**PPyV**) was synthesised as previously reported.^{38, 49, 50}

Instrumentation:

NMR spectroscopy: ¹H NMR spectra were recorded at room temperature on a Bruker Avance-400 NMR spectrometer at an operating frequency of 400 MHz. Samples were dissolved in a 50/50 v/v mixture of D₂O/*d*₂-formic acid. Chemical shifts are reported in parts per million (ppm).

UV/Vis absorbance: UV/Vis absorption spectra were recorded at room temperature on a Varian Cary 50 spectrometer.

Photoluminescence measurements: PL measurements were performed at room temperature with a Horiba Jobin Yvon SPEX Fluorolog- τ 3 fluorimeter (model FL-321, 450 W Xenon lamp) using right-angle conformation for solution-based measurements, and front-face conformation for thin films. Thin films were prepared by spin coating solutions of the respective solutions (**PPyV**: 10 mg/mL in 50/50 v/v H₂O/formic acid ; **PPyV-CB[7]**: 10 mg/mL of **PPyV** (ratio 20:1 **PPyV** r.u.:**CB[7]**) in 50/50 v/v H₂O/formic acid) at 3000 rpm for 1 min, following by overnight drying in a vacuum oven at 60 °C.

Acknowledgements:

This work was supported in part by the Irish Fulbright Commission and the National Science Foundation DMR-1410718. NWF thanks the Irish Research Council for a Government of Ireland postgraduate studentship.

References:

1. L. Huo, T. Lui, X. Sun, Y. Cai, A. J. Heeger and Y. Sun, *Adv. Mater.*, 2015, **27**, 2938-2944.
2. J.-S. Wu, S.-W. Cheng, Y.-J. Cheng and C.-S. Hsu, *Chem. Soc. Rev.*, 2015, **44**, 1113-1154.
3. C. Duan, K. Zhang, X. Guan, C. Zhong, H. Xie, F. Huang, J. Chen, J. Peng and Y. Cao, *Chem. Sci.*, 2013, **4**, 1298-1307.
4. P. Zalar, Z. B. Henson, G. C. Welch, G. C. Bazan and T.-Q. Nguyen, *Angew. Chem. Int. Ed.*, 2012, **51**, 7495-7498.
5. H. N. Kim, Z. Guo, W. Zhu, J. Yoon and H. Tian, *Chem. Soc. Rev.*, 2011, **40**, 79-93.
6. S. Rochat and T. M. Swager, *ACS Appl. Mater. Interfaces*, 2013, **5**, 4488-4502.
7. Q. Zhou and T. M. Swager, *J. Am. Chem. Soc.*, 1996, **117**, 7017-7018.
8. X. Feng, L. Liu, S. Wang and D. Zhu, *Chem. Soc. Rev.*, 2010, **39**, 2411-2419.
9. S. Hussain, A. H. Malik, M. A. Afroz and P. K. Iyer, *Chem. Commun.*, 2015, **51**, 7207-7210.
10. Y. Salinas, R. Martinez-Manez, M. D. Marcos, F. Sancenon, A. M. Costero, M. Parra and S. Gil, *Chem. Soc. Rev.*, 2012, **41**, 1261-1296.
11. T. M. Swager, *Acc. Chem. Res.*, 1998, **31**, 201-207.

12. A. Babel and S. A. Jenekhe, *J. Am. Chem. Soc.*, 2003, **125**, 13656-13657.
13. D. Izuhara and T. M. Swager, *J. Am. Chem. Soc.*, 2009, **131**, 17724-17725.
14. Y. Kim, J. E. Whitten and T. M. Swager, *J. Am. Chem. Soc.*, 2005, **127**, 12122-12130.
15. A. P. Kulkarni, C. J. Tonzola, A. Babel and S. A. Jenekhe, *Chem. Mater.*, 2004, **16**, 4556-4573.
16. S. Rochat and T. M. Swager, *J. Am. Chem. Soc.*, 2013, **135**, 17703-17706.
17. S. Rochat and T. M. Swager, *Angew. Chem. Int. Ed.*, 2014, **53**, 9792-9796.
18. L. Hu, F. Wu, C. Li, A. Hu, X. Hu, Y. Zhang, L. Chen and Y. Chen, *Macromolecules*, 2015, **48**, 5578-5586.
19. I. A. Adams and P. A. Rugar, *Macromol. Rapid Commun.*, 2015, **36**, 1336-1340.
20. Y. Takeda, T. L. Andrew, J. M. Lobe, A. J. Mork and T. M. Swager, *Angew. Chem. Int. Ed.*, 2012, **51**, 9042-9046.
21. P. A. Gale and C. Caltagirone, *Chem. Soc. Rev.*, 2015, **44**, 4212-4227.
22. M. J. Langton and P. D. Beer, *Acc. Chem. Res.*, 2014, **47**, 1935-1949.
23. G. P. Moss, P. A. S. Smith and D. Tavernier, *Pure & Appl. Chem.*, 1995, **67**, 1307-1375.
24. S. F. van Dongen, S. Cantekin, J. A. Elemans, A. E. Rowan and R. J. Nolte, *Chem. Soc. Rev.*, 2014, **43**, 99-122.
25. M. Arunachalam and H. W. Gibson, *Prog. Poly. Sci.*, 2014, **39**, 1043-1073.
26. S. S. Zhu, P. J. Carroll and T. M. Swager, *J. Am. Chem. Soc.*, 1996, **118**, 8713-8714.
27. S. S. Zhu and T. M. Swager, *J. Am. Chem. Soc.*, 1997, **119**, 12568-12577.
28. J. Lagona, P. Mukhopadhyay, S. Chakrabarti and L. Isaacs, *Angew. Chem. Int. Ed.*, 2005, **44**, 4844-4870.
29. E. Masson, X. Ling, R. Joseph, L. Kyeremeh-Mensah and X. Lu, *RSC Adv.*, 2012, **2**, 1213-1247.
30. F. Biedermann and W. M. Nau, *Angew. Chem. Int. Ed.*, 2014, **53**, 5694-5699.
31. M. Florea and W. M. Nau, *Angew. Chem. Int. Ed.*, 2011, **50**, 9338-9342.
32. W. Jiang, Q. Wang, I. Linder, F. Klautzsch and C. A. Schalley, *Chem. Eur. J.*, 2011, **17**, 2344-2348.

33. M. E. Haouaj, M. Luhmer, Y. H. Ko, K. Kim and K. Bartik, *J. Chem. Soc., Perkin Trans. 2*, 2001, 804-807.
34. M. E. Haouaj, Y. Ho Ko, M. Luhmer, K. Kim and K. Bartik, *J. Chem. Soc., Perkin Trans. 2*, 2001, 2104-2107.
35. L. Zhu, H. Yan, X. J. Wang and Y. Zhao, *J. Org. Chem.*, 2012, **77**, 10168-10175.
36. M. Fathalla, N. L. Strutt, J. C. Barnes, C. L. Stern, C. Ke and J. F. Stoddart, *Eur. J. Org. Chem.*, 2014, **2014**, 2873-2877.
37. M. Megyesi, L. Biczok and I. Jablonkai, *J. Phys. Chem. C*, 2008, **112**, 3410-3416.
38. J. W. Blatchford, T. L. Gustafson, A. J. Epstein, D. A. Vanden Bout, J. Kerimo, D. A. Higgins, P. F. Barbara, D.-K. Fu, T. M. Swager and A. G. MacDiarmid, *Phys Rev B*, 1996, **54**, R3684.
39. H. D. Burrows, S. M. Fonseca, C. L. Silva, A. A. C. C. Pais, M. J. Tapia, S. Pradhan and U. Scherf, *Phys. Chem. Chem. Phys.*, 2008, **10**, 4420-4428.
40. I. Ghosh, A. Mukhopadhyay, A. L. Koner, S. Samanta, W. M. Nau and J. N. Moorthy, *Phys. Chem. Chem. Phys.*, 2014, **16**, 16436-16445.
41. Z. Miskolczy, L. Biczok, M. Megyesi and I. Jablonkai, *J. Phys. Chem. B*, 2009, **113**, 1645-1651.
42. R. H. Herber and Y. Maeda, *Inorg. Chem.*, 1981, **20**, 1409-1415.
43. D. Tuncel, O. Ozsar, H. B. Tiftik and B. Salih, *Chem. Commun.*, 2007, 1369-1371.
44. M. Sayed, M. Sundararajan, J. Mohanty, A. C. Bhasikuttan and H. Pal, *J. Phys. Chem. B*, 2015, **119**, 3046-3057.
45. C. Marquez, R. R. Hudgins and W. M. Nau, *J. Am. Chem. Soc.*, 2004, **126**, 5806-5816.
46. C. Marquez and W. M. Nau, *Angew. Chem. Int. Ed.*, 2001, **40**, 3155-3160.
47. S. Liu, C. Ruspic, P. Mukhopadhyay, S. Chakrabarti, P. Y. Zavalij and L. Isaacs, *J. Am. Chem. Soc.*, 2005, **127**, 15959-15967.
48. L. Isaacs, *Acc. Chem. Res.*, 2014, **47**, 2052-2062.
49. M. J. Marsella, D.-K. Fu and T. M. Swager, *Adv. Mater.*, 1995, **7**, 145-147.

50. J. Tian, C. C. Wu, M. E. Thompson, J. C. Sturm, R. A. Register, M. J. Marsella and T. M. Swager, *Adv. Mater.*, 1995, **7**, 395-398.